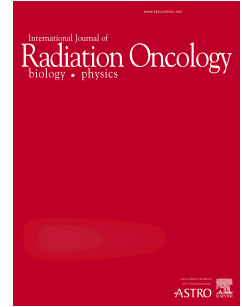


# Journal Pre-proof



The olfactory bulb provides a radioresistant niche for glioblastoma cells

Cindy R. Timme, PhD, Charlotte Degorre-Kerbaul, PhD, Joseph H. McAbee, BS, Barbara H. Rath, PhD, Xiaolin Wu, PhD, Kevin Camphausen, MD, Philip J. Tofilon, PhD

PII: S0360-3016(20)30066-3

DOI: <https://doi.org/10.1016/j.ijrobp.2020.01.007>

Reference: ROB 26150

To appear in: *International Journal of Radiation Oncology • Biology • Physics*

Received Date: 24 October 2019

Revised Date: 10 January 2020

Accepted Date: 13 January 2020

Please cite this article as: Timme CR, Degorre-Kerbaul C, McAbee JH, Rath BH, Wu X, Camphausen K, Tofilon PJ, The olfactory bulb provides a radioresistant niche for glioblastoma cells, *International Journal of Radiation Oncology • Biology • Physics* (2020), doi: <https://doi.org/10.1016/j.ijrobp.2020.01.007>.

This is a PDF file of an article that has undergone enhancements after acceptance, such as the addition of a cover page and metadata, and formatting for readability, but it is not yet the definitive version of record. This version will undergo additional copyediting, typesetting and review before it is published in its final form, but we are providing this version to give early visibility of the article. Please note that, during the production process, errors may be discovered which could affect the content, and all legal disclaimers that apply to the journal pertain.

Published by Elsevier Inc.

**The olfactory bulb provides a radioresistant niche for glioblastoma cells**

Cindy R. Timme, PhD, Charlotte Degorre-Kerbaul, PhD, Joseph H. McAbee, BS, Barbara H. Rath, PhD, Xiaolin Wu, PhD, Kevin Camphausen, MD and Philip J. Tofilon, PhD

Radiation Oncology Branch, National Cancer Institute, Bethesda, Maryland, USA (CRT, CD-K, JHM, BHR, KC, PJT)

Department of Clinical Neurosciences, University of Cambridge, Cambridge, UK (JM)

Wake Forest University School of Medicine, Winston-Salem, North Carolina, USA (JM)

Cancer Research Technology Program, Frederick National Laboratory for Cancer Research, Leidos Biomedical Research, Inc., Frederick, Maryland, USA (XW)

**Running Title:** Olfactory bulb provides a radioresistant niche

**Corresponding Author:**

Philip J. Tofilon, PhD

Senior Investigator

National Cancer Institute

Radiation Oncology Branch

10 Center Drive-MSB 1002

Building 10, B3B69B

Bethesda, MD 20892

Email: philip.tofilon@nih.gov

Phone: (240) 858-3048

**Statistical analyses:** Cindy Timme

**Funding:** Division of Basic Sciences, Intramural Program, National Cancer Institute (Z1ABC011372). This project has also been funded in part with Federal funds from the National Cancer Institute, National Institutes of Health, under Contract No. HHSN261200800001E. The content of this publication does not necessarily reflect the views or policies of the Department of Health and Human Services, nor does mention of trade names, commercial products, or organizations imply endorsement by the U.S. Government.

**The authors declare no potential conflicts of interest**

**Acknowledgement:** All microscopy was performed with the aid of Ross Lake of the Laboratory of Genitourinary Cancer Pathogenesis Microscopy Core Facility, NCI, NIH.

**Running Title:** Olfactory bulb provides a radioresistant niche

## **Abstract**

**Background:** The various microenvironments existing within the brain combined with the invasive nature of glioblastoma (GBM) creates the potential for a topographical influence on tumor cell radiosensitivity. The aim of this study was to determine whether specific brain microenvironments differentially influence tumor cell radioresponse.

**Methods:** GBM stem-like cells (GSCs) were implanted into the right striatum of nude mice. To measure radiosensitivity, proliferation status of individual tumor cells was determined according to the incorporation of 5-chloro-2'-deoxyuridine delivered at 4, 8, 12 and 20 days after brain irradiation. As an additional measure of radiosensitivity, the %human cells in the right hemisphere and the olfactory bulb were defined using ddPCR. Targeted gene expression profiling was accomplished using NanoString analysis.

**Results:** Tumor cells were detected throughout the striatum, corpus callosum and olfactory bulb. After an initial loss of proliferating tumor cells in the corpus callosum and striatum after irradiation, there was only a minor recovery by 20 days. In contrast, the proliferation of tumor cells located in the olfactory bulb began to recover at 4 days and returned to unirradiated levels by day 12 post-irradiation. Defining the %human cells in the right hemisphere and the olfactory bulb after irradiation also suggested that the tumor cells in the olfactory bulb were relatively radioresistant. Gene expression profiling identified consistent differences between tumor cells residing in the olfactory bulb versus the right hemisphere.

**Conclusion:** These results suggest that the olfactory bulb provides a radioresistant niche for GBM cells.

## Introduction

Glioblastoma (GBM) has long been classified as a radioresistant tumor<sup>1-3</sup>. Whether this treatment outcome reflects a homogeneous radioresponse among the cells comprising a given GBM or is dictated by a radioresistant subpopulation(s) remains unclear. The presence of tumor cell subpopulations of varying radiosensitivities would have implications not only in the development of more effective radiotherapy but also the application of molecularly targeted radiosensitizers.

The radioresponse of brain tumor models is typically evaluated according to animal survival and more recently using imaging techniques to define tumor growth rate, both of which describe the radiosensitivity of the tumor cell population as a whole. To identify variations in radiosensitivity among the subpopulations of a given tumor, it is necessary to evaluate radioresponse at the individual cell level. Towards this end, one approach is to deliver halogenated thymidine analogs after irradiation followed by histochemical analysis. Halogenated thymidine analogs are incorporated into DNA during the S-phase of the cell cycle; this procedure has long been used to identify proliferating cells in normal tissue and tumors<sup>4</sup>. With respect to radioresponse, incorporation of the halogenated thymidine analog after irradiation would be indicative of proliferation with such cells classified as radioresistant. The histology-based identification of cells that do and do not proliferate after irradiation thus provides a strategy for defining intratumor heterogeneity in radiosensitivity.

GBMs *in situ* are highly migratory and extensively invasive<sup>5</sup>, resulting in tumor cells being distributed across the multiple microenvironmental niches that exist within the brain. Consequently, a potential source of intratumor heterogeneity in radiosensitivity among the cells

of a given GBM is the location at the time of irradiation. To investigate the role of specific brain microenvironments in determining tumor cell radioresponse, we used orthotopic xenografts initiated from GBM stem-like cells (GSCs). GSCs are thought to be critical to the development, maintenance and treatment response of GBM<sup>6</sup>. Moreover, GSC-initiated orthotopic xenografts not only replicate the genotype and phenotype of GBMs but also their *in vivo* growth pattern<sup>7,8</sup>. In the study described here, GSCs implanted into the right striatum are shown to migrate into the frontal cortex and olfactory bulb (OB). The data presented indicate that tumor cells in the OB were radioresistant as compared to those in the corpus callosum (CC) and striatum. Thus, these results suggest that the murine OB provides a radioresistant niche for tumor cells.

## Materials and Methods

**Cell Lines:** The glioblastoma stem-like cell (GSC) lines NSC11 and NSC20 (provided by Dr. Frederick Lang, MD Anderson Cancer Center) were maintained as neurospheres; CD133+ GSCs were isolated by FACS<sup>9</sup> and met the criteria for tumor stem-like<sup>9,10</sup>. *In vitro* clonogenic survival analysis was performed as described<sup>9</sup>.

**Orthotopic Xenografts:** GSCs ( $1.0 \times 10^5$ ), transduced to express luciferase and GFP with the lentivirus LVpFUGQ-UbC-ffLuc2-eGFP2 were implanted into the right striatum of 6-week-old athymic female nude mice (NCI Animal Production Program, Frederick, MD)<sup>11</sup>. Before irradiation mice were randomized according to the bioluminescent imaging signal (BLI)<sup>11</sup>. 5-chloro-2'-deoxyuridine (CldU) was delivered by daily intraperitoneal (IP) injections (100mg/kg) with mice euthanized 2h after the last injection. For irradiation, mice were anesthetized and placed in plexi glass jigs with shielding for the entire torso of the mouse along with critical normal structures of the head. Radiation was delivered using an X-Rad 320 X-

irradiator (Precision X-Rays, Inc) at 2.9 Gy/min. All experiments were performed as approved by the principles and procedures in the NIH Guide for Care and Use of Animals and conducted in accordance with the Institutional Animal Care and Use Committee.

**Immunohistochemical analysis:** Formalin fixed brains were embedded in paraffin and cut into 6-10 $\mu$ m sections. The antibodies used were: human SOX2 (Cell Signaling), CldU (clone BU1/75, ICR1), phospho-H2AX (Millipore), anti-rabbit-AlexaFluor488, anti-rat-AlexaFluor647 and anti-mouse-AlexaFluor555. Image analysis is described in Supplementary Methods.

**Digital Droplet PCR (ddPCR):** Copy numbers of a human gene (Myocardin-like protein 2 (MKL2)) and a mouse gene (Transferrin Receptor (Tfrc)) were determined by ddPCR and used to calculate the ratio of human/mouse cells (Supplementary methods).

**NanoString nCounter Gene Expression:** Using paraffin blocks generated from brain tumors on day 35 post-implant, RNA was isolated from core punches (1.5-2mm diameter) with the RNease FFPE kit (Qiagen). RNA (200ng) was analyzed using the NanoString nCounter Human PanCancer and Human Neuropath gene expression panels (NanoString Technologies) and nSolver analysis software according to NanoString guidelines<sup>12</sup>. Differentially expressed genes (OB vs. right hemisphere) were defined as  $p < 0.05$  (Student's *t*-test). Classification into Gene Ontologies was performed using Panther (<http://pantherdb.org/>) and pathway enrichment analyses were performed using Ingenuity Pathway Analysis (IPA®, QIAGEN).

## Results

To evaluate the radiosensitivity of human tumor cells as a function of location within the murine brain, orthotopic xenografts were generated from CD133+ NSC11 GSCs. At day 28 post-implantation, CldU was delivered for 2-6 days; mice were euthanized 2h after the last

injection, and brains collected for immuno-histochemical analysis of CldU incorporation to identify cycling cells with co-staining for SOX2 to identify the NSC11 cells in the mouse background. The survival of unirradiated mice after NSC11 implantation is approximately 55 days<sup>13</sup>. SOX2 expression was detected in the right striatum (implantation site), corpus callosum (CC) and cortex as well as the left hemisphere (figure 1A). The specificity of SOX2 staining for human tumor cells is illustrated in Supplemental Figure 1. CldU<sup>+</sup> tumor cells were detectable after 2 days of injections with an increase in the percentage of tumor cells (SOX<sup>+</sup>) expressing CldU at 4 days. Higher magnification of SOX2<sup>+</sup> and CldU<sup>+</sup> cells (figure 1B) was used for the quantification of CldU<sup>+</sup> tumor cells. CldU was detected in approximately 50% of tumor cells in the right striatum and CC after 2 days, which increased to >80% after 6 days (figure 1C). These results indicate the xenografts contain a large fraction of cycling cells.

This procedure was then applied to irradiated tumors. On day 35 post-implantation, NSC11 brain tumors received 10Gy; on days 4, 12 and 20 after irradiation CldU delivery was initiated (3 daily IP injections with tumors collected 2h after the last dose). The 4day delay between irradiation and the first CldU injection was chosen to allow for the resolution of the presumed initial transient cell cycle arrest. At the specified times after irradiation immuno-histochemical analyses of CldU incorporation and SOX2 expression was performed to determine the percentage of tumor cells that were proliferating in the CC, striatum and OB (figure 2A). SOX2 staining in the sagittal section of the right hemisphere from a control mouse (figure 2A top panel) shows that by day 35 after implantation, NSC11 cells had migrated into the frontal cortex and to the right OB.

When CldU injections were initiated 12 days after irradiation there was a reduction in CldU<sup>+</sup> tumor cells in the CC and striatum (bottom panel, figure 2A). However, in the OB, the

level of CldU+ tumor cells in the irradiated mice was similar to that in the unirradiated animals. The %CldU+ tumors in each location as a function of time after 10Gy is shown in figure 2B. When CldU was delivered at 4 days post-10Gy, less than 4% of tumor cells in the CC and striatum were CldU+, levels that increased slightly when CldU delivery was initiated 20 days after irradiation. In the OB, whereas there was considerable variability among mice at 4 days post-10Gy, the %CldU+ tumor cells was similar to controls at 12 days increasing above controls at 20 days post-10Gy. Thus, while there was some recovery of tumor cell proliferation in the CC and striatum 20 days after irradiation, recovery of NSC11 cells in the OB was faster and more complete. These initial results suggest that tumor cells in the OB are relatively radioresistant.

As an orthogonal approach to comparing radiosensitivity of tumor cells in the OB versus the right hemisphere, ddPCR was used to determine the number of copies of a human specific gene (*MKL2*) and a mouse specific gene (*Tfrc*) in each region, which provides a measure of the %human cells. On days 35, 42 and 49 after implantation of NSC11 cells into the right striatum, the right OB and right hemisphere were collected by gross dissection of GFP-expressing tumor tissue; DNA was isolated from each region and the %human cells determined. In addition, 8 mice were irradiated (10Gy) on day 35 and their right OB and right hemisphere collected on days 42 and 49 post-implant, respectively. The %human cells increased in the unirradiated OB and right hemisphere over the 14 days analysis period (figure 2C), consistent with tumor cell proliferation. After 10Gy, the %human cells in the right hemisphere declined over the 14day period. In contrast, in the OB the %human cells was slightly increased at 14 days after 10Gy. These results, consistent with those generated from the analysis of CldU+ cells, indicate that NSC11 cells in the OB are radioresistant as compared to those in the right hemisphere.

As an estimation of *in vivo* dosimetry,  $\gamma$ H2AX foci<sup>14</sup>, were defined in the CC, striatum and OB. Mice were irradiated and  $\gamma$ H2AX foci scored in SOX2 expressing cells in each location at 0.5 and 6h post-irradiation. Representative images generated from the OB are shown in figure 3A.  $\gamma$ H2AX foci/cell levels in each location 0.5h after irradiation (figure 3B) were similar indicating that there was no difference in the initial level of radiation-induced DSBs in OB compared to the CC or striatum and that each location received an equivalent radiation dose.

To further investigate the microenvironment as a determinant of tumor cell radiosensitivity, neurosphere cultures were generated from the OB and the right hemisphere of 2 mice bearing NSC11 tumors (35 days post-implant) and subjected to *in vitro* clonogenic survival analyses<sup>9</sup>. For each mouse the radiation survival curves generated from NSC11 cells isolated from the OB and right hemisphere were similar (Figure 3C). These data suggest that the radioresistance of NSC11 cells in the OB is dependent on the continued input from the microenvironment.

The analysis of tumor cell proliferation based on CldU incorporation was then extended to the orthotopic xenografts initiated from the NSC20 GSCs using the same treatment protocol as for NSC11 tumors. On day 35 post-implantation, NSC20 brain tumor xenografts were exposed to 10Gy; on days 4 and 12 after irradiation CldU delivery was initiated (3 daily IP injections with tumors collected 2h after the last dose). As shown by the SOX2 expression in the control tumors (figure 4A), by day 35 after implantation, although there remain NSC20 cells in the striatum, many have invaded past the CC and into the cortex. The percentage of CldU+ tumor cells was similar between frontal cortex and striatum. Although the growth pattern was different from that of NSC11 in the right hemisphere, NSC20 cells also infiltrated the OB (figure 4A, right panel).

When CldU injections were initiated 12 days after irradiation there was a dramatic loss of CldU+ tumor cells throughout the right hemisphere (bottom panel, figure 4A). However, in the OB, the level of CldU+ tumor cells in the irradiated mice was similar to that in the control animals. Quantitation of the %CldU+ tumor cells after irradiation (figure 4B) shows a significant reduction in the right hemisphere at 4 and 12 days after 10Gy. In the OB, whereas there was considerable variability among mice at 4 days, the %CldU+ tumor cells returned to control levels by 12 days post-10Gy. These data indicate that NSC20 cells in the OB are relatively radioresistant as compared to those in the right hemisphere. As for NSC11 tumors, ddPCR was used to determine the %human cells in the OB and right hemisphere after irradiation. After 10Gy the %human cells in the right hemisphere declined over the 14day analysis period, whereas the %human cells in the OB slightly increased. These results, consistent with the CldU analysis, indicate that NSC20 cells in the OB are relatively radioresistant as compared to those in the right hemisphere.

To compare the molecular phenotype of the NSC11 tumor cells residing in the OB and the right hemisphere, targeted gene expression profiling was performed on RNA isolated from FFPE samples using the NanoString nCounter Analysis System, which provided a quantitative expression analysis of 1385 genes. Comparison of gene expression levels in the OB versus right hemisphere identified 233 differentially expressed genes ( $p < 0.05$ ) (Supplemental figure 2A, Supplemental Table 1). These significant genes were organized into Gene Ontologies and the classification of “GO biological process complete” was used to annotate the pathways. Table 1 lists examples of the significantly overexpressed pathways that were nested within *Cellular Process* to *Chemical Synaptic Transmission* (FDR range 2.95E-15 to 3.36E-25). This gene list was interrogated using Ingenuity Pathway Analysis (IPA). The majority of genes (158/233)

were present under the KEGG heading *Nervous System Development and Function* with 49 sub-headings related to the nervous system each of which was significant ( $p < 10E-13$ ). The networked genes within these headings ( $n=135$ ) are shown in figure 5A with most genes increased (red) in the tumors harvested from the OB compared to the right hemisphere. Within this network are multiple genes that correspond to calcium metabolism, glutamate receptors and BMPs.

Performing the same gene expression analysis on NSC20 cells in the OB versus the right hemisphere identified 199 significant genes (Supplemental figure 2B, Supplemental Table 2). The differentially expressed genes distributed to a similar set of GO pathways associated with neuronal function as with the NSC11 tumors, with all but *Synaptic Transmission, glutamatergic* being significant (Table 1). Genes from the NSC20 tumors in the OB also sorted to *signal transduction (GO:0007165)* in a more significant way than NSC11. When the NSC20 outliers were subjected to IPA the majority of genes also appeared under the KEGG heading *Nervous System Development and Function*. The networked genes ( $n=63$ ) within this heading are shown in figure 5B. The genes that were differentially expressed ( $n=34$ ) between tumor cells in the OB and right hemisphere for both NSC20 and NSC11 included BMPs, calcium metabolism and glutamate receptors (Supplemental figure 3).

## Discussion

The assortment of microenvironments that exist within the brain combined with the invasive nature of GBM creates the potential for a topographical influence on tumor cell biology. In experimental models GSCs have been reported to preferentially locate in a number of niches including perivascular and perineuronal<sup>15</sup>. Although noteworthy with respect to the

fundamental biology of GBM, whether a given location preferentially impacts tumor cell radiosensitivity has yet to be determined. To address this issue, we used GSCs that after orthotopic implantation migrate throughout the mouse brain. Results generated from 2 experimental approaches showed that tumor cells in the OB are radioresistant as compared to those in the right hemisphere. These data indicate that the murine OB provides a radioresistant niche for tumor cells. More broadly, these results illustrate the potential for intratumor heterogeneity in GBM radiosensitivity.

Whether the OB in the human brain provides an analogous niche is unclear. However, defining the molecular and cellular processes that mediate the radioresistance in murine OB may generate a better understanding of the mechanisms responsible for the radioresistance of GBM in general. Along these lines, recent studies have identified a direct interaction between neurons and glioma cells, which, based on single cell transcriptome analysis, resulted in the modification of glioma gene expression and, moreover, were implicated as a source of tumor progression<sup>16,17</sup>. The murine OB is highly enriched in neurons and interneurons providing an environment that may promote neuron-glioma cell interactions. Accordingly, as recently reported for single cell transcriptomes<sup>16,17</sup>, targeted expression analysis comparing the NSC11 and NSC20 cells in the murine OB and right hemisphere showed that the tumor cells residing in the OB preferentially expressed genes related to neuronal function. Thus, whereas defining the molecular and cellular processes that mediate radioresponse of tumor cells in murine OB may provide an opportunity to investigate a radioresistant subpopulation, it may also lead to a better understanding of the mechanisms responsible for the radioresistance of GBM in general.

## References

1. Stupp R, Mason WP, van den Bent MJ, et al. Radiotherapy plus concomitant and adjuvant temozolomide for glioblastoma. *N Engl J Med*. 2005; 352(10):987-996.
2. Chan JL, Lee SW, Fraass BA, et al. Survival and failure patterns of high-grade gliomas after three-dimensional conformal radiotherapy. *J Clin Oncol*. 2002; 20(6):1635-1642.
3. Laperriere N, Zuraw L, Cairncross G, Cancer Care Ontario Practice Guidelines Initiative Neuro-Oncology Disease Site G. Radiotherapy for newly diagnosed malignant glioma in adults: a systematic review. *Radiother Oncol*. 2002; 64(3):259-273.
4. Vega CJ, Peterson DA. Stem cell proliferative history in tissue revealed by temporal halogenated thymidine analog discrimination. *Nat Methods*. 2005; 2(3):167-169.
5. Giese A, Bjerkvig R, Berens ME, Westphal M. Cost of migration: invasion of malignant gliomas and implications for treatment. *J Clin Oncol*. 2003; 21(8):1624-1636.
6. Venere M, Fine HA, Dirks PB, Rich JN. Cancer stem cells in gliomas: identifying and understanding the apex cell in cancer's hierarchy. *Glia*. 2011; 59(8):1148-1154.
7. Lee J, Kotliarova S, Kotliarov Y, et al. Tumor stem cells derived from glioblastomas cultured in bFGF and EGF more closely mirror the phenotype and genotype of primary tumors than do serum-cultured cell lines. *Cancer Cell*. 2006; 9(5):391-403.
8. Vescovi AL, Galli R, Reynolds BA. Brain tumour stem cells. *Nat Rev Cancer*. 2006; 6(6):425-436.
9. Blinded for review
10. Blinded for review
11. Blinded for review
12. Kulkarni MM. Digital multiplexed gene expression analysis using the NanoString nCounter system. *Curr Protoc Mol Biol*. 2011; Chapter 25:Unit25B 10.
13. Blinded for review

14. Bonner WM, Redon CE, Dickey JS, et al. GammaH2AX and cancer. *Nat Rev Cancer*. 2008; 8(12):957-967.
15. Silver DJ, Lathia JD. Revealing the glioma cancer stem cell interactome, one niche at a time. *J Pathol*. 2018; 244(3):260-264.
16. Venkataramani V, Tanev DI, Strahle C, et al. Glutamatergic synaptic input to glioma cells drives brain tumour progression. *Nature*. 2019; 573(7775):532-538.
17. Venkatesh HS, Morishita W, Geraghty AC, et al. Electrical and synaptic integration of glioma into neural circuits. *Nature*. 2019; 573(7775):539-545.

### Figure Legends

**Figure 1. CldU incorporation into NSC11 xenografts.** On day 28 post-implantation daily CldU treatment was initiated (100mg/kg, IP) with mice euthanized 2h after the last injection. A) Representative coronal images collected after 2 and 4 days of CldU delivery. B) Representative high magnification images. C) CldU+ tumor cells in each location (right hemisphere) as a function of the days of CldU treatment. Each point corresponds to an individual mouse with at least 200 cells analyzed (mean $\pm$ SEM for 4-5 mice).

**Figure 2. NSC11 cell proliferation after brain irradiation.** 35days post-implant, mice received 10Gy; CldU delivery (3 daily doses with the tumor collected 2h after the last dose) was initiated on the specified day after irradiation. CldU delivery was initiated to control mice on day 35. A) Representative matched images of sagittal sections of the right hemisphere and

coronal sections of the right OB of a control mouse (top) and a mouse in which CldU delivery was initiated on day 12 post-10Gy (bottom). (CC: Corpus Callosum; STR: Striatum; HIP: Hippocampus; GL: Glomerular Layer; GCL: Granule Cell Layer). B) CldU+ tumor cells identified in the CC, STR and OB of matched mice as a function of time after 10Gy. Each point corresponds to an individual mouse (mean $\pm$ SEM for 3-4 mice), \*p<0.05 vs. control. (C) %human cells in the right OB and corresponding right hemisphere (RH) as a function of time after 10Gy. Mice were collected on day 0 (day 35 post-implant) or received 10Gy and collected for analysis 7 and 14days later along with unirradiated controls. Values represent the mean  $\pm$  SEM of 4 mice, \*p<0.05 vs. day 35, Student's t-test.

**Figure 3.  $\gamma$ H2AX foci in NSC11 xenografts and in vitro radiosensitivity of NSC11 GSCs isolated from olfactory bulb and right hemisphere.** On day 35 post-implant of NSC11 cells, mice received 6Gy and collected for analysis at the indicated time points. A) Representative images of  $\gamma$ H2AX foci in tumor cells (SOX2+) (40x magnification). The last column corresponds to the overlay used for automated foci counting. B)  $\gamma$ H2AX foci in the CC, striatum and OB as a function of time after 6Gy. Each column corresponds to an individual mouse with at least 50 cells analyzed per mouse at each location. Bars represent mean  $\pm$  SEM. C) . Two NSC11 tumor bearing mice were euthanized on day 35 post-implant. GFP fluorescent tissue was collected from the OB and right hemisphere from each mouse, disaggregated and seeded into standard tissue culture plates in stem cell media. The resulting neurospheres grown from each location were subjected to in vitro clonogenic survival analysis. Values represent the mean  $\pm$  SD of 3 independent experiments.

**Figure 4. NSC20 cell proliferation after brain irradiation.** 35days post-implant, mice received 10Gy; CldU delivery (3 daily doses with the tumor collected 2h after the last dose) was initiated on the specified days after irradiation. CldU delivery was initiated to control mice on day 35. A) Representative matched images of sagittal sections of the right hemisphere and coronal sections of the right OB of a control mouse and a mouse in which CldU delivery was initiated on day 12 post-10Gy. Insets: zoomed-in images illustrating cells in the right hemisphere. B) CldU+ tumor cells identified in the RH and OB of matched mice as a function of time after 10Gy. Each point corresponds to an individual mouse with at least 200 cells analyzed in each location (mean $\pm$ SEM for 3-4 mice) \* $p$ <0.05 vs. control. (D) %human cells in the right OB (OB) and corresponding RH as a function of time after 10Gy. Mice were collected on day 35 (day 0) or received 10Gy and collected for analysis 7 and 14days later along with unirradiated controls. Values represent the mean  $\pm$  SEM of 4-8 mice, \* $p$ <0.05 vs. day 35.

**Figure 5. Gene expression for tumor cells growing in the OB versus the right hemisphere.** IPA networked genes under the KEGG heading *Nervous System Development and Function* for A) NSC11 and B) NSC20. Shades of red refer to up-regulated genes in the OB and green to down regulated genes. The color intensity of a molecule indicates the degree of increased or decreased enrichment. Other colors indicate the presence (gray) or absence (white) of a given gene.

**TABLE 1.** Biological/biochemical functions of the genes differentially expressed in NSC11 and NSC20 cells growing in the olfactory bulb versus the right hemisphere.

GO Pathway	NSC11			NSC20		
	Genes Expected	Genes Detected	FDR	Genes Expected	Genes Detected	FDR
Cellular Process (0009987)	69	152	3.36E-25	141	199	5.77E-23
└ Cell Communication (0007154)	6	42	8.33E-20	52	147	1.10E-38
└ Cell-Cell Signaling (0007267)	6	42	7.95E-18	11	54	1.49E-20
└ Synaptic Signaling (0099536)	4	30	2.32E-15	4	22	7.58E-08
└ Trans-synaptic Signaling (0099537)	4	30	2.55E-15	4	21	1.44E-07
└ Anterograde trans-synaptic sig (0098916)	4	30	2.63E-15	4	20	3.67E-07
└ Chemical Synaptic transmission (0007268)	4	30	2.95E-15	4	20	3.68E-07
└ Synaptic Transmission, glutamatergic (0035249)	0.5	12	1.25E-10	0.5	1	8.64E-01
└ Cell Surface receptor signaling (1905114)	23	103	1.01E-30	23	103	1.29E-38
└ Wnt Signaling (0016055)	4	17	2.93E-05	4	17	4.42E-06
└ Signal Transduction (0007165)	19	82	9.39E-27	49	133	2.55E-32
└ Cell surface receptor signaling (0007166)	8	44	7.14E-17	23	103	1.29E-38
└ Glutamate receptor signaling (0007215)	0.5	12	3.98E-11	0.5	5	2.29E-03
└ MAPK cascade (0000165)	4	20	4.56E-10	4	18	1.57E-06

**TABLE 1.** Biological/biochemical functions of the genes differentially expressed in NSC11 and NSC20 cells growing in the olfactory bulb versus the right hemisphere.

	NSC11			NSC20		
GO Pathway	Genes Expected	Genes Detected	FDR	Genes Expected	Genes Detected	FDR
Cellular Process (0009987)	69	152	3.36E-25	141	199	5.77E-23
└Cell Communication (0007154)	6	42	8.33E-20	52	147	1.10E-38
└└Cell-Cell Signaling (0007267)	6	42	7.95E-18	11	54	1.49E-20
└└└Synaptic Signaling (0099536)	4	30	2.32E-15	4	22	7.58E-08
└└└└Trans-synaptic Signaling (0099537)	4	30	2.55E-15	4	21	1.44E-07
└└└└└Anterograde trans-synaptic sig (0098916)	4	30	2.63E-15	4	20	3.67E-07
└└└└└└Chemical Synaptic transmission (0007268)	4	30	2.95E-15	4	20	3.68E-07
└└└└└└└Synaptic Transmission, glutamatergic (0035249)	0.5	12	1.25E-10	0.5	1	8.64E-01
└└└Cell Surface receptor signaling (1905114)	23	103	1.01E-30	23	103	1.29E-38
└└└└Wnt Signaling (0016055)	4	17	2.93E-05	4	17	4.42E-06
└└Signal Transduction (0007165)	19	82	9.39E-27	49	133	2.55E-32
└└└Cell surface receptor signaling (0007166)	8	44	7.14E-17	23	103	1.29E-38
└└└└Glutamate receptor signaling (0007215)	0.5	12	3.98E-11	0.5	5	2.29E-03
└└└└└MAPK cascade (0000165)	4	20	4.56E-10	4	18	1.57E-06

Figure 1

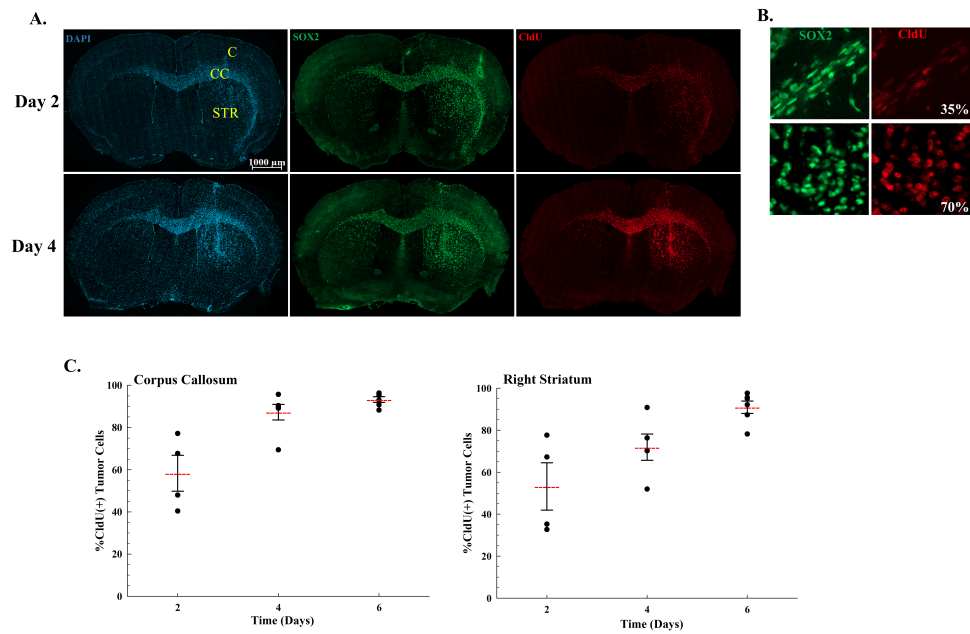


Figure 2

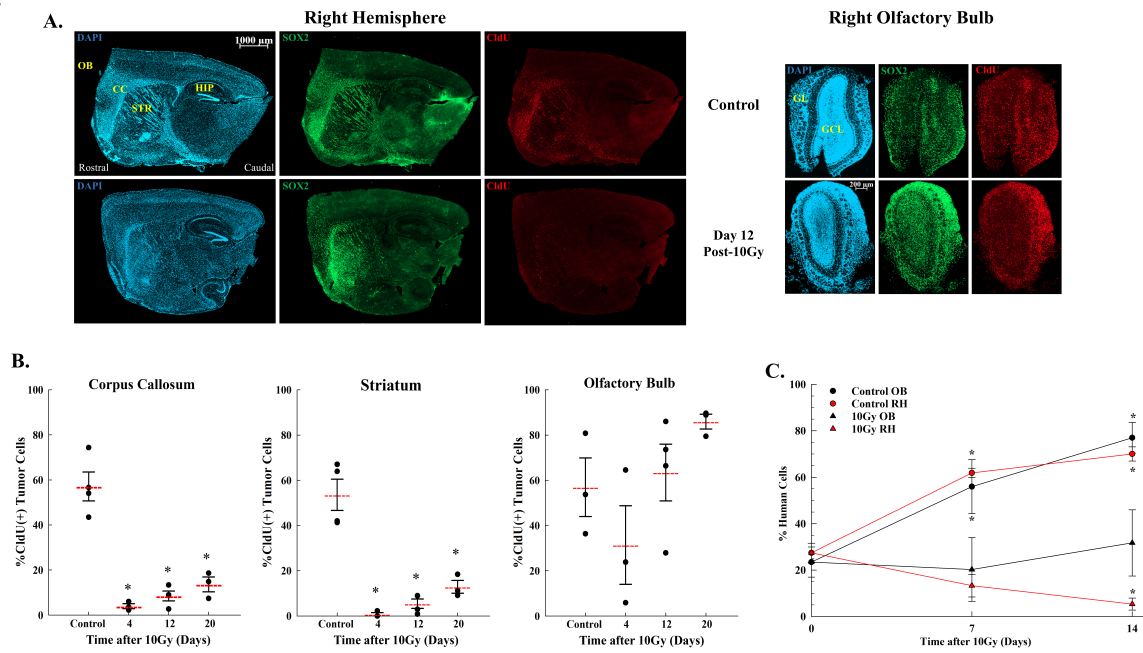


Figure 3

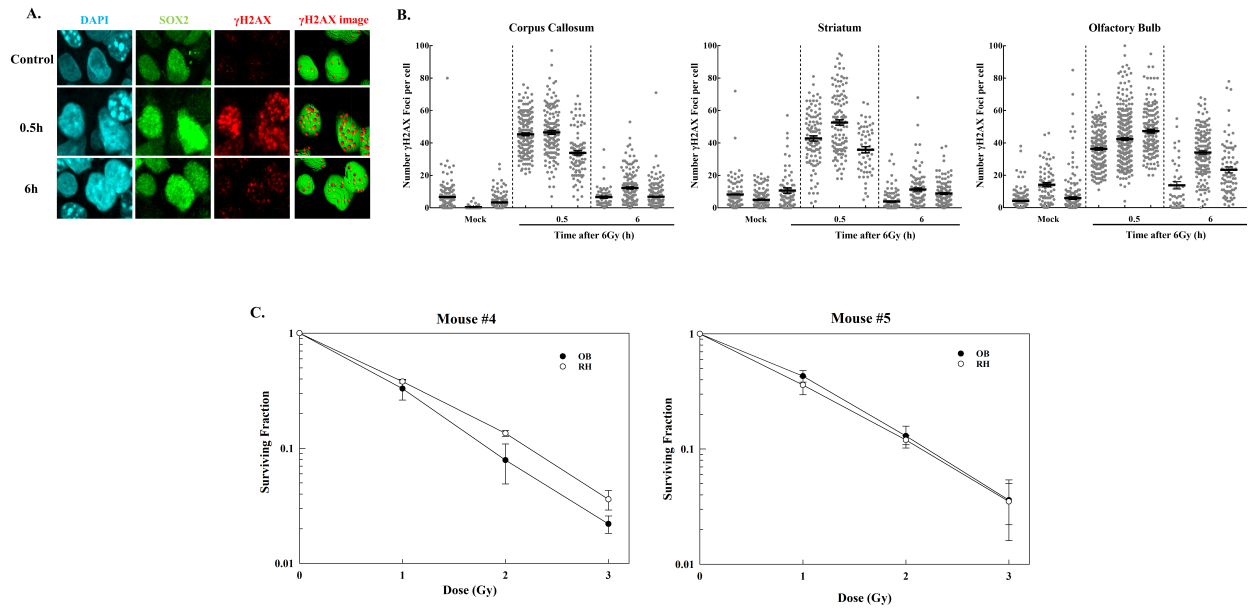


Figure 4

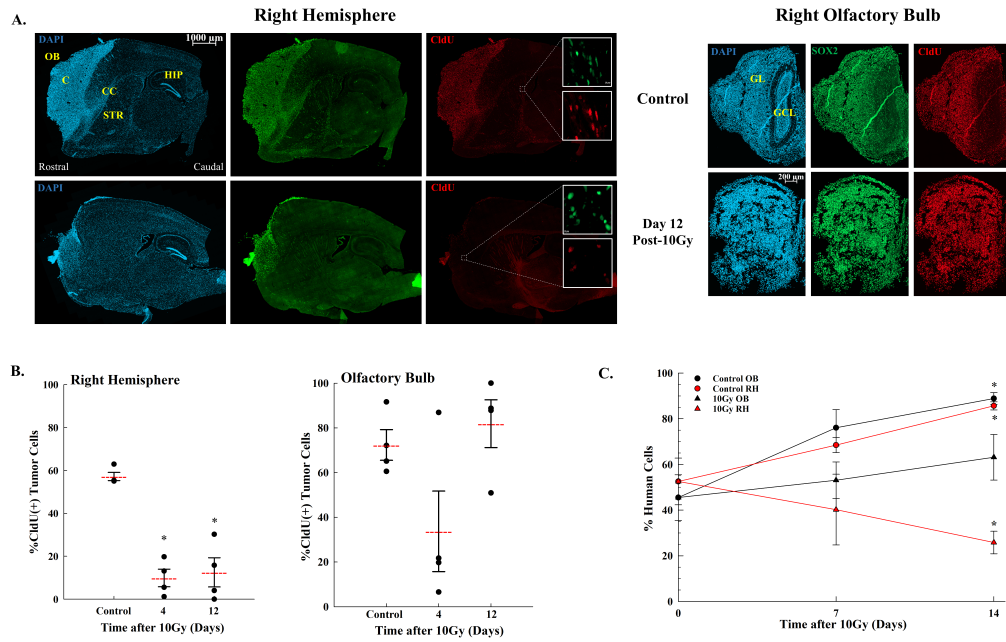
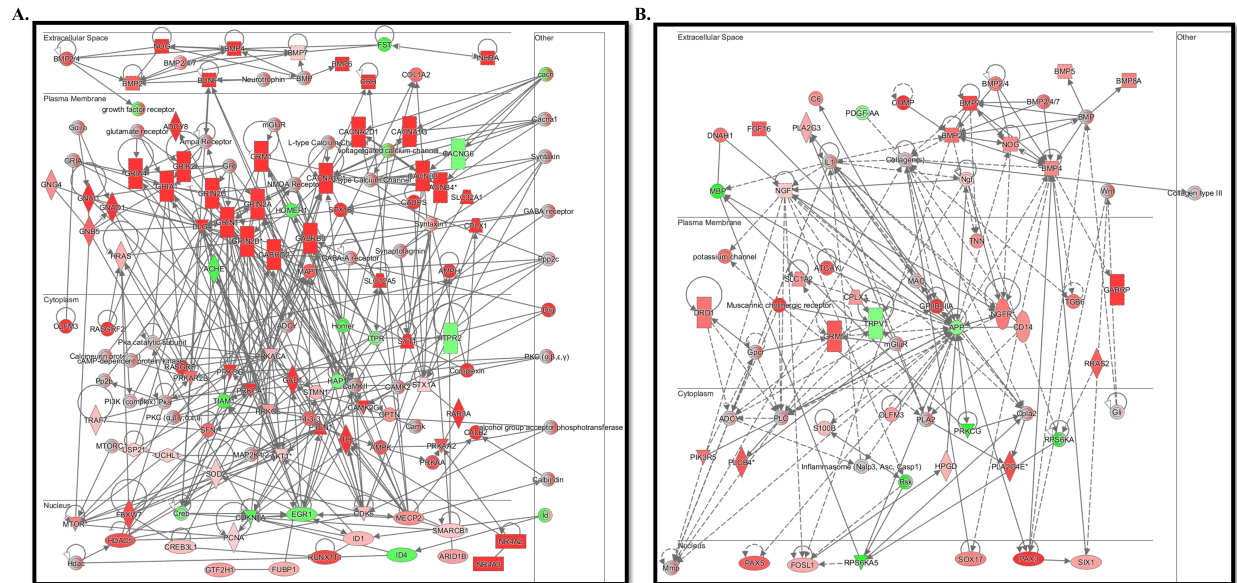


Figure 5



Journal Pre